COMMUNICATION

Check for updates

Additive manufacturing of high-performance polycyanurates *via* photo-induced catalytic poly-trimerization†

Raffael Wolff, [ID] [a] Patrick Knaack, [ID] [a] Konstanze Seidler, [ID] [b] Christian Gorsche, [ID] [b] Thomas Koch, [ID] [c] Jürgen Stampfl [ID] [c] and Robert Liska [ID] *[a]

Polycyanurates offer outstanding thermomechanical properties due to their unique triazine structure in combination with phenolic chains. Generally, these resistant thermosets are formed into the desired shape *via* lengthy molding processes. With the aid of photo-induced catalytic poly-trimerization, not only the photochemical curing of cyanate esters can be described here, but also the production of pure polycyanurates by employing an additive manufacturing variant, the Hot Lithography. Other methods in the field of additive manufacturing of this class of thermosets relied on matrix polymers or fillers for less precise printing variants. The presented reaction process could be monitored *via* photo-DSC and IR, and the thermomechanical properties could be analyzed by simultaneous thermal analysis and dynamic mechanical analysis. The presented formulation is stable under the selected conditions for 3D printing at elevated temperatures, showing sufficient reactivity. The thermomechanical values obtained for the 3D printed structures are in regions that have rarely been attainable for additive manufacturing using laser-induced curing. Together with the commonly used high chemical resistance, this proof-of-concept process offers an extraordinary opportunity for the production of high-performance polymers for additive manufacturing.

Communication/letter

Additive manufacturing is considered as one of the most promising engineering solutions for the production of highly complex components in various application areas.[1] Whether in the medical field,[2,3] in aerospace,[4–6] or in the automotive industry,[7,8] this technology is exploited everywhere to achieve results that were previously not possible with such ease. In order for this process to become even more effectively implemented in industrial applications, research must be conducted in all areas of additive manufacturing. Especially in the field of micrometer-precise polymer parts for high temperature applications, the options of choice are still relatively limited. The method of choice for micrometer-scale manufacturing of components is photopolymer-based printing using stereolithography (SLA).[9] For high temperature mechanical resistance, epoxides[10] or complex modified systems such as acrylated benzoxazines[11] or methacrylated bismaleimides[9] with a glass transition temperature (T_g) of 150–260 °C are utilized as SLA resins on a scientific basis. Another class of high-temperature resins are cyanate esters. The cyclotrimerization of the cyanate groups forms triazine rings, which give the resulting polycyanurate network exceptional mechanical properties, as well as a low dielectric constant, low moisture absorption and tremendous thermal properties.[12,13] For this type of polymerization, a catalytic center of transition metals (*i.e.* iron or manganese) is often chosen to lower the reaction temperature. Additionally, a co-catalyst can be used to provide an active hydrogen which accelerates the reaction.[14,15] Fig. 1a shows the reaction mechanism of the poly-trimerization. After coordination of the cyanate group around the catalytic metal center (in this case, iron), trimerization to the triazine is started with the help of the proton of the cocatalyst. Carboxylates of the various transition metals are commonly used as such catalysts for curing.[14] However, Kotch *et al.* showed that by illuminating a formulation of 1,1-bis(cyanatophenyl)ethane and photolabile iron–arene complexes, a reduced reaction temperature of the curing peak can be achieved and photo-induced catalytic poly-trimerization is feasible.[16] Previous attempts to use polycyanurates in additive manufacturing processes were carried out *via* matrix polymers and incorporation in an interpenetrating network ($T_g \sim 240$ °C)[17] or *via* direct ink writing of a thixotropic formulation filled with silica particles ($T_g \sim 280$ °C).[18] Theoretically, depending on the cyanate ester used, T_g's in the range between 300 and 400 °C are possible.[19] For pure curing of cyanate esters with catalysts, temperatures in the

[a]Institute of Applied Synthetic Chemistry, Technische Universität Wien, Getreidemarkt 9/163 MC, 1060 Vienna, Austria. E-mail: robert.liska@tuwien.ac.at

[b]Cubicure GmbH, Gutheil-Schoder Gasse 17, Tech Park Vienna, 1230 Vienna, Austria

[c]Institute of Materials Science and Technology, Technische Universität Wien, Getreidemarkt 9/308, 1060 Vienna, Austria

† Electronic supplementary information (ESI) available. See DOI: https://doi.org/10.1039/d3ta01264f

This journal is © The Royal Society of Chemistry 2023

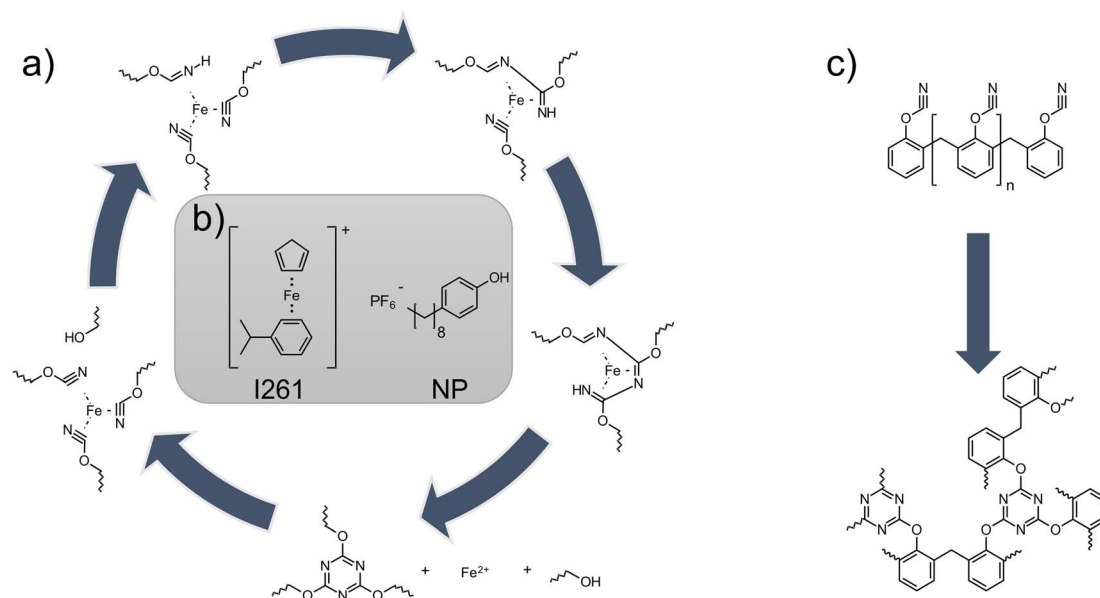*J. Mater. Chem. A*, 2023, 11, 10545–10550 | **10545**

Fig. 1 (a) Reaction mechanism of catalytic curing of cyanate esters to polycyanurates (adapted from ref. 13). (b) The catalyst system employed, consisting of I261 and NP. (c) Reaction of cyanate ester PT-30 to the final network.

range of higher than 90 °C are usually required with post-curing cycles up to 260 °C to reach the final T_g's.[20] Consequently, using the commercial photoinitiator (cumene)cyclopentadienyl iron(II) hexafluorophosphate (former Irgacure 261, I261, Fig. 1b left) together with an active hydrogen donor such as non-ylphenol (NP, Fig. 1b right), photocatalytic curing at elevated temperatures should be possible and therefore enable cyanate ester to be used in applications such as lithography based additive manufacturing.

The additive manufacturing technology required for this approach is Hot Lithography.[21] Using a heated vat and platform, various new materials can be 3D printed layer-by-layer, which was not possible before, including oxazolines,[22] lactones,[23] bakelite®[24] and furan-based resins.[25] In this article, by exploiting this technique with the system previously described, we show that we have been able to expand the possibilities of 3D printing by adding a category in the high-performance range, with the disadvantage for applications that have a sensitivity to iron atoms, since for the formulation presented here, the coordinative center remains in the cured product.

For the theoretical investigation of the cyanurates, a mono-functional reactant, phenyl cyanate, was used for the initial experiments (Scheme S1†). Upon irradiation at 100 °C using photo-DSC, the formulation with 1 wt% I261 along with 5 wt% NP gave an exothermic enthalpy of 610 J g^{-1}. The structure of the photo product was analyzed via ^{1}H and ^{13}C-NMR (Fig. S1–S4†) and compared to literature values[26] as well as the molecular weight was determined by UPLC-MS to be 357 g mol^{-1}, which equals the molecular weight of the desired trimerization product. Furthermore, a conversion of 86% of the phenyl cyanate was detected by HPLC. Considering the mass fractions of the resin, as well as the mass losses during polymerization because of the evaporation of volatile monomer a value of 74

kJ mol^{-1} per equivalent cyanate group can be calculated (eqn (S1)†). This is within the range of values given in the literature (78 ± 3).[27]

The photo-DSC measurement (Fig. 2a) of the commercial functionalized novolak resin PT-30 (Fig. 1c) with the same proportions of the photoinitiator as well as the co-catalyst showed values of 240–300 J g^{-1} for the heat of trimerization depending on the temperature. The time until the maximum of the heat evolution (t_{max}) is between 18 and 22 s (Fig. S2†). Based on the monofunctional framework and assuming that the number of functional cyanates group equals the repeating unit of the resin (131 g per equiv.), this results in trimerization conversion values from 45 ± 2% at 80 °C to 55 ± 3% at 100 °C (Fig. 2b & eqn (S2)†). Nevertheless, all illuminated samples were solid, non-meltable and insoluble in various solvents, regardless of the temperature during irradiation. The reaction speeds are in a range that can be considered suitable for additive manufacturing. Both t_{max} and the rate of polymerization (R_p, eqn (S3)†) improve significantly with higher temperature, effectively demonstrating that high temperatures facilitate the 3D printing of pure cyanate ester resins. It has to be noted that measurements without I261 gave no enthalpy at all, while measurements without NP released less than 100 J g^{-1} of energy and did not become solid.

In the literature, infrared spectroscopy (IR) is often utilized instead of DSC to monitor the conversion of the reaction to form the thermosets, since the values of the theoretical enthalpy of the OCN groups vary over and in part between the different monomers.[28] In order to obtain the latter, the C≡N stretching vibrations at 2270 and 2235 cm^{-1} are integrated and quantified with reference to the methyl C–H stretching vibrations of the side chain at 2970 cm^{-1} (Fig. 3a).[15,28,29] In addition, the formation of the triazine network via the triazine ring C≡N stretching

10546 | J. Mater. Chem. A, 2023, **11**, 10545–10550

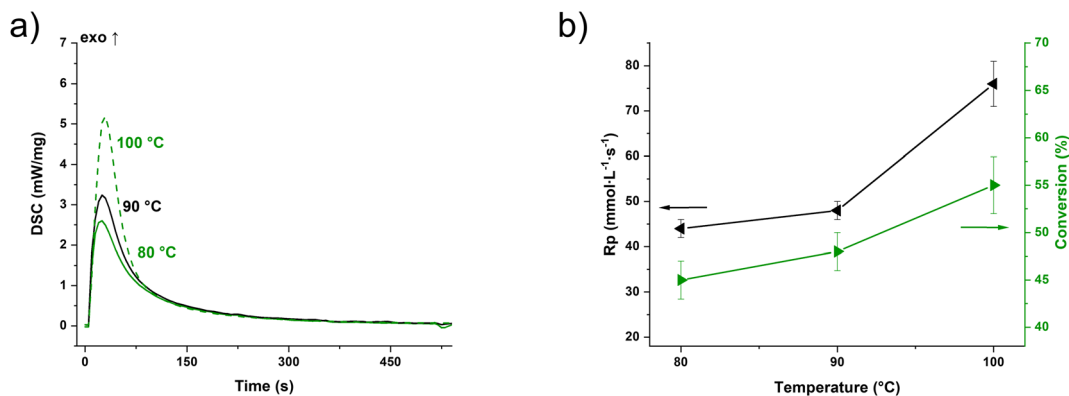This journal is © The Royal Society of Chemistry 2023

Fig. 2 (a) Photo-DSC of the PT-30 formulation at 80–100 °C, 2 × 900 s, 320–500 nm, 60 mW cm⁻². (b) Temperature dependence of rate of polymerization (R_p black) and conversion of the cyanate ester groups (green).
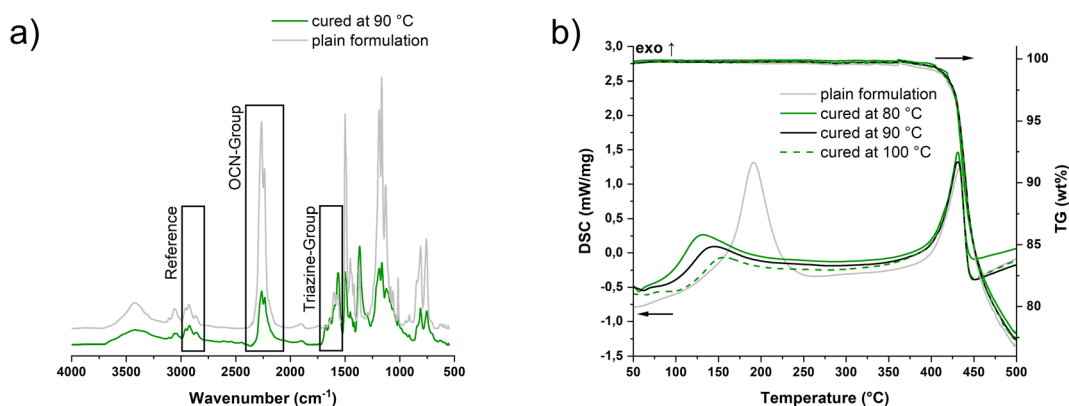

Fig. 3 (a) IR spectra of the plain formulation (grey) and the sample cured at 90 °C (green). (b) STA of the plain formulation (grey) and the photo-DSC cured samples at 80 °C (green solid), 90 °C (black solid) and 100 °C (green dot).

vibration at 1565 cm⁻¹ can be observed qualitatively.[30] Thus, conversions ranging from $50 \pm 2\%$ at 80 °C to $58 \pm 2\%$ at 100 °C were obtained (Table S2†). The consistency with the results from the photo-DSC can be considered as good.

Furthermore, the irradiated specimens were subjected to a post-curing program recommended by the manufacturer (Fig. S5†).[31] Here, the conversion could be increased to maximal $86 \pm 2\%$. Accordingly, the lower the temperatures in the initial irradiation process the lower the final conversions. The benefits of post-hardening could also be demonstrated by means of creep tests of the purely thermally hardened materials (Fig. S7†). The specimens with post-curing already show initially less elongation at a load of 5 MPa and, as the load progresses, significantly higher stability compared to the specimens without post-curing. This is also evident in the creep modulus over time (Fig. S8†).

In the simultaneous thermogravimetric analysis (STA), the trend observed in the photo-DSC was confirmed. Measuring the photo-cured samples as well as the pure formulation, it could be detected that the higher the temperature during the initial irradiation process, the higher the conversion, the lower the remaining exotherm in the samples (Fig. 3b). Furthermore, the observation noted by Kotch *et al.* can be confirmed, which

showed a reduced onset temperature for previously irradiated formulations with iron–arene complexes. Compared to the pure thermal curing of the resin, preliminary irradiation of the samples at elevated temperatures lowers the onset of the exothermic peak from 160 °C to the range of 90–110 °C, depending on the temperature during irradiation. Regardless, it can be noted that I261 can also be used as a pure thermal catalyst comparing the onset of the pure formulation to the temperatures otherwise used for curing without a catalyst (>240 °C).[32] Moreover, the material obtained *via* light-induced curing shows no difference from the thermal degradation compared to the purely thermally cured material. The onset of 426 °C for degradation is slightly lower than those of conventionally cured PT-30 samples,[33] but comparable to those of the 3D printed samples *via* DIW by Chandrasekaran *et al.*[18]

In order to be suitable for the printing process using Hot Lithography, the formulation must be stable for a long period of time at the selected printing temperature. For this purpose, the formulation was monitored for 2 h at 100 °C in the STA to see if the components of the formulation are not too volatile. No weight loss could be observed in this case (Fig. S7†). Furthermore, part of the formulation was stored in an oven at 100 °C for several days and its viscosity was regularly measured to observe

This journal is © The Royal Society of Chemistry 2023

J. Mater. Chem. A, 2023, **11**, 10545–10550 | **10547**

a progressive reaction to indicate the long-term stability of the formulation. Starting from a viscosity of 0.1 Pa s, which is well within the window of Hot Lithography (<20 Pa s (ref. 21)), the viscosity increases to 3.5 Pas within 72 h. This indicates that the formulation is sufficiently stable for the Hot Lithography process. Meanwhile, formulations without NP or without I261 show virtually no increase in viscosity over the period tested (Fig. S8†).

The demonstrated stability of the formulation as well as the possibility of photoinduced catalytic poly-trimerization made this system a good candidate for use in Hot Lithography. A printing temperature of 90 °C and a printing speed of 1 m s^{-1} with 10 repetitions were selected, as well as a layer thickness of 50 μm. Previous irradiation tests under the same conditions without a building platform resulted in a potential layer thickness of 203 μm. In addition to DMA test specimens, a hollow cube was designed as the CAD model (Fig. 4a) and 3D printed as a proof-of-concept of the working system (Fig. 4b). Both printed structures were subjected to the post-curing program described earlier before imaging or further testing. As can be seen in the pictures, there is a slight overpolymerization during the printing process which was polished off for refinement of the mechanical test specimen. The overpolymerization can be assigned to the diffusion of the catalytic system. The scanning electron microscopy (SEM) images illustrate the structure in detail, in particular the layer thickness of 50 μm, which can be tuned very well despite the visible overpolymerization (Fig. 4c). Delamination between the printed layers induced by the post-processing program was not observed.

Ultimately, the DMA specimens produced via Hot Lithography were tested for their thermomechanical properties in 3-point bending mode and compared with specimens that had been purely thermally cured with the same formulation. All samples were subjected to the same standard post-curing process (Fig. 4d). Both, the purely thermally cured (4350 ± 200 MPa) and the 3D printed (3650 ± 100 MPa) samples, show a storage modulus at 25 °C in the range or slightly higher in comparison to the values given in the literature (3580 MPa).[34] Comparing the two samples in terms of T_g, there is an increased T_g for the 3D printed samples to 336 ± 5 °C compared to 305 ± 5 °C for the thermally cured samples. Usually, this indicates that I261 is less active as a thermal catalyst than the
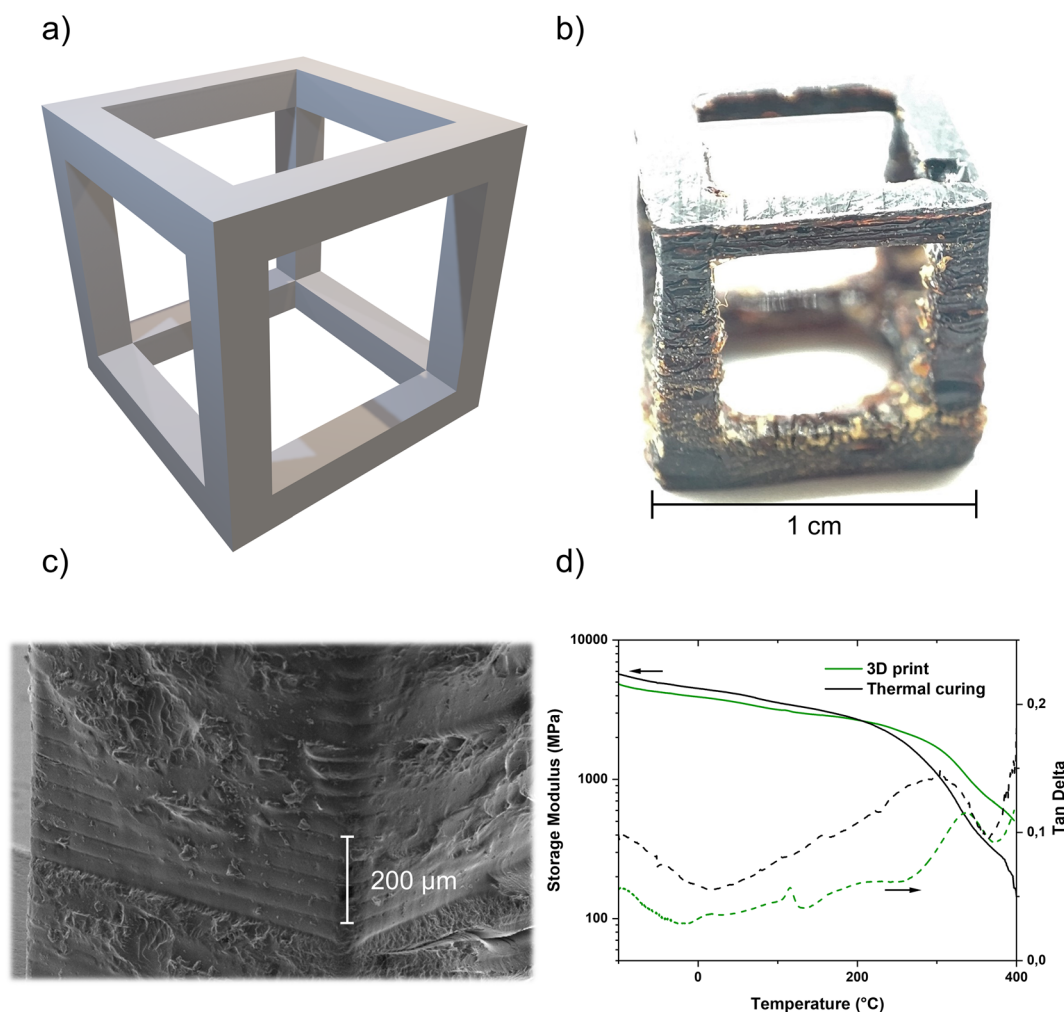

Fig. 4 (a) CAD model of the hollow cube. (b) 3D printed and post-cured hollow cube. (c) SEM image of the 3D printed structure. (d) DMA tests in the 3-point bending mode: storage modulus (solid) and tan delta (dot) of the 3D printed (green) and thermally (black) cured samples.

10548 | J. Mater. Chem. A, 2023, 11, 10545–10550

This journal is © The Royal Society of Chemistry 2023

combination of photo and thermal initiation. That could lead to a lower crosslinking density and therefore to a lower T_g. This could be usually determined by the height of the rubbery plateau. As the samples start to decompose already in the range around 400 °C, the lower crosslinking density could not be confirmed. Only the course of the curve indicates a higher rubber plateau of the 3D printed sample and thus a higher crosslinking density. In addition, the determination of the conversion *via* IR of the purely thermally cured materials generally shows a conversion that is about 5% lower than that of the photo-chemically cured samples, even in the post-cured stage (Table S2†). Nevertheless, the T_g of the 3D printed sample is still lower than values from the literature or by the manufacturer (up to 400 °C).[31,34] However, these are obtained from curing pure PT-30, without a catalyst or co-catalyst, which can reduce the crosslinking density. Regardless, the T_g of 336 °C is one of the highest T_g's ever reported for an unfilled photo-polymerized material in the field of laser-based additive manufacturing.

Conclusion

By combining a photolabile initiator as well as a co-catalyst in conjunction with a novolac-based cyanate ester derivative (PT-30), it was possible to prepare a pure polycyanurate by means of photo-induced catalytic poly-trimerization. The achieved conversions are sufficient to obtain a solid part, having excellent thermomechanical values in the course of post-processing. The formulation presented here made it possible to perform 3D printing by Hot Lithography and thus to demonstrate a successful proof-of-concept for the additive manufacturing of pure polycyanurates. With a T_g of 336 °C and a degradation onset of 426 °C, one of the most thermally stable unfilled systems ever cured by photopolymerization for additive manufacturing was obtained.

Conflicts of interest

There are no conflicts to declare.

Acknowledgements

Notes and references

1 S. C. Ligon, R. Liska, J. Stampfl, M. Gurr and R. Mülhaupt, *Chem. Rev.*, 2017, **117**, 10212–10290, DOI: **10.1021/ACS.CHEMREV.7B00074**.

2 J. W. Kim, B. E. Yang, S. J. Hong, H. G. Choi, S. J. Byeon, H. K. Lim, S. M. Chung, J. H. Lee and S. H. Byun, *Int. J. Mol. Sci.*, 2020, **21**, 4837, DOI: **10.3390/IJMS21144837**.

3 I. Karakurt, A. Aydoğdu, S. Çıkrıkcı, J. Orozco and L. Lin, *Int. J. Pharm.*, 2020, **584**, 119428, DOI: **10.1016/j.ijpharm.2020.119428**.

4 M. Hoffmann and A. Elwany, *J. Manuf. Sci. Eng.*, 2023, **145**(2), 1–22, DOI: **10.1115/1.4055603**.

5 E. Sacco and S. K. Moon, *Int. J. Adv. Manuf. Technol.*, 2019, **105**, 4123–4146, DOI: **10.1007/s00170-019-03786-z**.

6 S. A. Kumar, A. Pathania, A. Shrivastava, V. Rajkumar and P. Raghupatruni, *Nanotechnology-Based Addit. Manuf.*, 2023, pp. 561–578, DOI: **10.1002/9783527835478.CH19**.

7 R. Velu, F. Raspall and S. Singamneni, in *Green Compos. Automot. Appl.*, Woodhead Publishing, 2018, pp. 171–196.

8 N. Shahrubudin, T. C. Lee and R. Ramlan, in *Procedia Manuf.*, Elsevier, 2019, pp. 1286–1296.

9 W. Hua, Q. Lin, B. Qu, Y. Zheng, X. Liu, W. Li, X. Zhao, S. Chen and D. Zhuo, *Materials*, 2021, **14**, 1708, DOI: **10.3390/ma14071708**.

10 C. Dall'Argine, A. Hochwallner, N. Klikovits, R. Liska, J. Stampf and M. Sangermano, *Macromol. Mater. Eng.*, 2020, **305**, 2000325, DOI: **10.1002/mame.202000325**.

11 Y. Lu, K. W. J. Ng, H. Chen, X. Chen, S. K. J. Lim, W. Yan and X. Hu, *Chem. Commun.*, 2021, **57**, 3375–3378, DOI: **10.1039/d0cc07801h**.

12 W. Kern, R. Schröder, K. Hummel, C. Mayer and M. Hofstötter, *Eur. Polym. J.*, 1998, **34**, 987–995, DOI: **10.1016/S0014-3057(97)00209-7**.

13 M. R. Kessler, in *Wiley Encycl. Compos.*, John Wiley & Sons, Inc., Hoboken, NJ, USA, 2012, pp. 1–15.

14 T. Fang and D. A. Shimp, *Prog. Polym. Sci.*, 1995, **20**, 61–118, DOI: **10.1016/0079-6700(94)E0006-M**.

15 J. Bauer and M. Bauer, *Acta Polym.*, 1988, **39**, 548–551, DOI: **10.1002/actp.1988.010391004**.

16 T. G. Kotch, A. J. Lees, S. J. Fuerniss and K. I. Papathomas, *Chem. Mater.*, 1995, **7**, 801–805, DOI: **10.1021/cm00052a028**.

17 Z. X. Zhou, Y. Li, J. Zhong, Z. Luo, C. R. Gong, Y. Q. Zheng, S. Peng, L. M. Yu, L. Wu and Y. Xu, *ACS Appl. Mater. Interfaces*, 2020, **12**, 38682–38689, DOI: **10.1021/acsami.0c10909**.

18 S. Chandrasekaran, E. B. Duoss, M. A. Worsley and J. P. Lewicki, *J. Mater. Chem. A*, 2018, **6**, 853–858, DOI: **10.1039/c7ta09466c**.

19 Arxada, *Primaset™ Cyanate Ester Resins Leading Edge High Performance Thermoset Resins Product Manual*, 2022.

20 J. N. Hay, in *Chem. Technol. Cyanate Ester Resins*, Springer, Dordrecht, 1994, pp. 151–192.

21 M. Pfaffinger, *Laser Tech. J.*, 2018, **15**, 45–47, DOI: **10.1002/LATJ.201800024**.

22 N. Klikovits, L. Sinawehl, P. Knaack, T. Koch, J. Stampfl, C. Gorsche and R. Liska, *ACS Macro Lett.*, 2020, **9**, 546–551, DOI: **10.1021/ACSMACROLETT.0C00055**.

23 Y. Mete, P. Knaack and R. Liska, *Polym. Int.*, 2022, **71**, 797–803, DOI: **10.1002/pi.6326**.

24 R. Wolff, K. Ehrmann, P. Knaack, K. Seidler, C. Gorsche, T. Koch, J. Stampfl and R. Liska, *Polym. Chem.*, 2022, **13**, 768–777, DOI: **10.1039/d1py01665b**.

25 L. Pezzana, R. Wolff, G. Melilli, N. Guigo, N. Sbirrazzuoli, J. Stampfl, R. Liska and M. Sangermano, *Polymer*, 2022, **254**, 125097, DOI: **10.1016/j.polymer.2022.125097**.

26 H. Namazi and M. Adeli, *J. Polym. Sci., Part A: Polym. Chem.*, 2005, **43**, 28–41, DOI: **10.1002/POLA.20471**.

27 M. R. Pallaka and S. L. Simon, in *43rd North Am. Therm. Anal. Soc. Conf.*, Montreal, 2015.

This journal is © The Royal Society of Chemistry 2023

J. Mater. Chem. A, 2023, **11**, 10545–10550 | **10549**

28 S. L. Simon and J. K. Gillham, *J. Appl. Polym. Sci.*, 1993, **47**, 461–485, DOI: **10.1002/app.1993.070470308**.

29 D. A. Shimp and W. M. Craig, in *Int. SAMPE Symp. Exhib.*, Publ By SAMPE, 1989, pp. 1336–1346.

30 W. A. Heckle, H. A. Ory and J. M. Talbert, *Spectrochim. Acta*, 1961, **17**, 600–606, DOI: **10.1016/0371-1951(61)80120-3**.

31 Arxada, *Primaset™ PT-30 A Multifunctional Cyanate Ester Delivering High T_g and Inherent Flame Retardancy*, 2017.

32 C.-C. Chen, T.-M. Don, T.-H. Lin and L.-P. Cheng, *J. Appl. Polym. Sci.*, 2004, **92**, 3067–3079, DOI: **10.1002/app.20314**.

33 M. L. Ramirez, R. Walters, R. E. Lyon and E. P. Savitski, *Polym. Degrad. Stab.*, 2002, **78**, 73–82, DOI: **10.1016/S0141-3910(02)00121-0**.

34 A. Toldy, P. Niedermann, G. Szebényi and B. Szolnoki, *Express Polym. Lett.*, 2016, **10**, 1016–1025, DOI: **10.3144/expresspolymlett.2016.94**.

10550 | *J. Mater. Chem. A*, 2023, **11**, 10545–10550

This journal is © The Royal Society of Chemistry 2023